Supplemental Tables

Table S1. Primer sequences for *Tfpi*$^{fl/fl}$ *Pf4-Cre*$^{+}$ mice.

Primer	Sequences 5'-3'
P1	TCCCTCCCCACCAGTACTTC
P2	AGGACTCCGCCCTCTAATCC
Cre-1	CCCATACAGCACACCTTTTG
Cre-2	TGCACAGTCAGCAGGTT
+PCR-1	ACTGGGATCTTCGAACTCTTTGGAC
+PCR-2	GATGTTGGGGCACTGCTCATTCACC

Table S2. Complete blood counts from Tx-pltTFPIα^{neg} and Tx-pltTFPIα^{pos} mice.[1]

Blood Count Parameter	Tx-pltTFPIα^{neg} N=3	Tx-pltTFPIα^{pos} N=5	p-value
WBC Count (10^3/μL)	3.2±0.4	5.2±0.9	p=0.2761
RBC Count (10^6/μL)	7.3±0.1	7.5±1.1	p=0.9739
Hemoglobin (g/dL)	10.6±0.2	11.4±1.4	p=0.6417
Hematocrit (%)	32.3±0.4	38.2±5.2	p=0.1252
Platelet Count (10^3/μL)	802±206	895±211	p=0.8661

[1]Values for experimental mice were not different from those reported for similar aged mice at https://www.jax.org/-/media/jaxweb/files/jax-mice-and-services/phenotypic-data/aged-b6-physiological-data-summary.pdf?la=en&hash=F955A6EF778DB4F3390ECD2410DE9259A0F6DD50.

Table S3. Location of ventricular mural clots.

Location	Tx-pltTFPIα^{neg} N=12	Tx-pltTFPIα^{pos} N=6
Right Side	33%	0%
Left Side	8%	0%
Both Sides	50%	0%
No Clots	8%	100%

Supplemental Figures

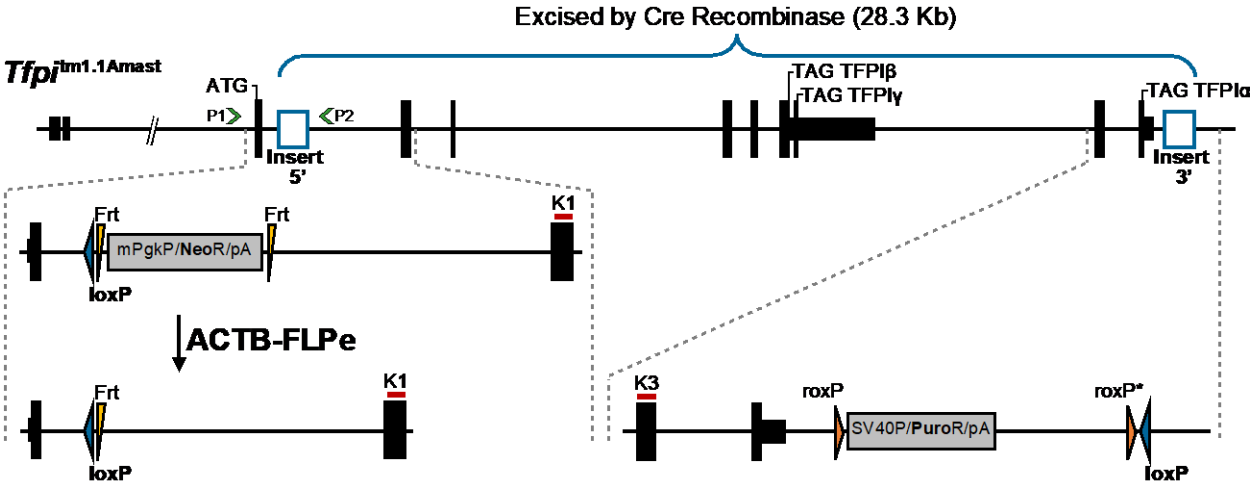

Supplemental Figure 1: Schematic of the conditional total *Tfpi* KO allele.
LoxP sites were targeted to the *Tfpi* gene locus using a two-construct approach. Grey hash lines indicate magnified genomic regions. A 5'-end construct (Insert 5') targeted a single loxP site between the first and second coding exons of the *Tfpi* gene (containing the ATG start site and the K1 domain, respectively). This 5' construct contained a neomycin (Neo) positive selection cassette flanked by Frt sites for selective germline deletion by FLPe recombinase. The 3'-end construct (Insert 3') targeted a second, single loxP site to an intergenic region ~1 kb downstream of the TFPIα-encoding terminal exon and ~57 kb upstream of the neighboring *Calcrl* gene. This 3' construct contained the puromycin (Puro) positive selection marker flanked by roxP sites for selective deletion by Dre recombinase. The 5' and 3' constructs were electroporated into C57BL/6N ES cells for homologous recombination and karyotyped ES cell clones incorporating the targeting vector were microinjected into Balb/C embryos and implanted into pseudo-pregnant Balb/C female mice. Founders were confirmed to carry an initial *Tfpi*^{tm1Amast} conditional allele by sanger sequencing over the 5' and 3' inserted sequences. Sequencing additionally identified mutations in the 3'-most roxP site (roxP*) rendering it non-functional for Dre-mediated recombination and removal of the Puro cassette. *Tfpi*^{tm1Amast} founders were outcrossed to ACTB-FLPe mice to excise the Neo cassette generating the final *Tfpi*$^{tm1.1Amast}$ (*Tfpi*^{fl}) conditional total KO allele. Progeny derived from a single male founder were maintained for this mouse line. This allele is WT expressing until rendered inactive by Cre-mediated excision of the 28.3 kb of genomic sequence containing exons encoding all 3 kunitz domains and all TFPI isoform specific terminal exons (indicated by TAG stop codon). Green arrowheads indicate positions of P1 and P2 germline genotyping primers used to differentiate the *Tfpi* WT allele from the *Tfpi*^{fl} haploblock after FLPe-mediated excision of the neo cassette.

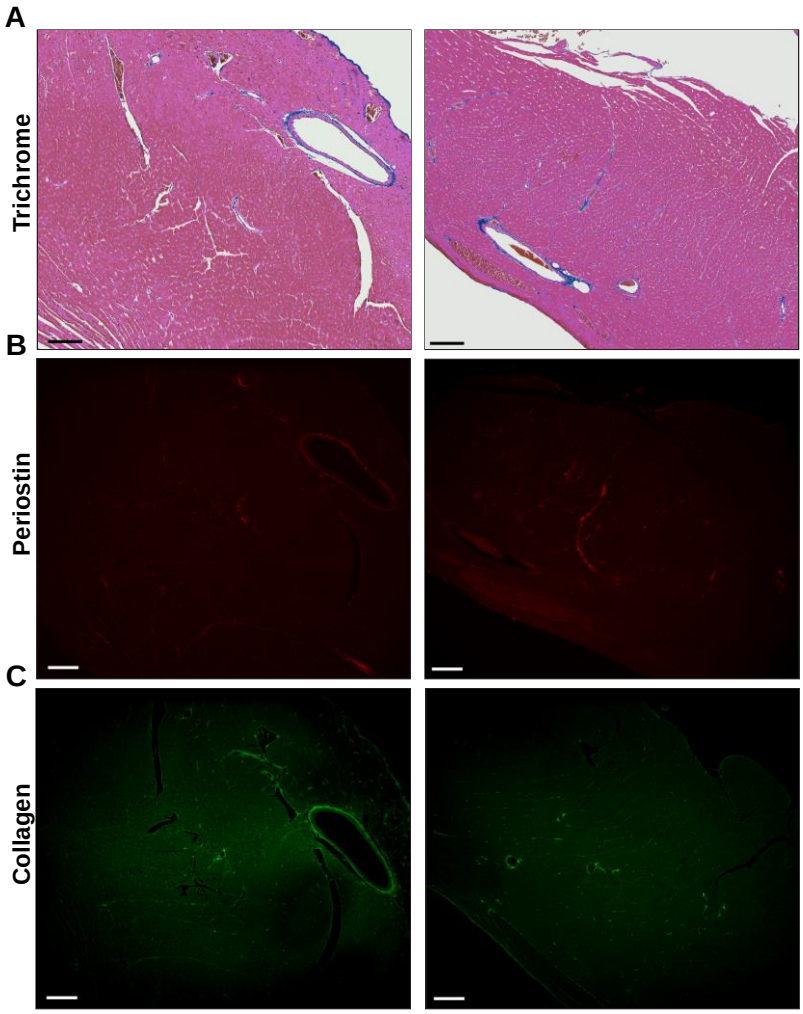

Supplemental Figure 2: The *Tfpi*$^{fl/fl}$ *Pf4-Cre*$^{+}$ donor mice did not have cardiac thrombosis or fibrosis. The heart tissue from two *Tfpi*$^{fl/fl}$ *Pf4-Cre*$^{+}$ mice was evaluated using (A) Trichrome stain, (B) periostin immunohistochemistry (fluorescent emission 647, red), and (C) Picrosirius red fluorescent stain (fluorescent emission 568, green) to delineate cardiac clot formation, fibroblast activation, and increased collagen production, respectively. No significant pathological lesions were observed (bar=100μm).

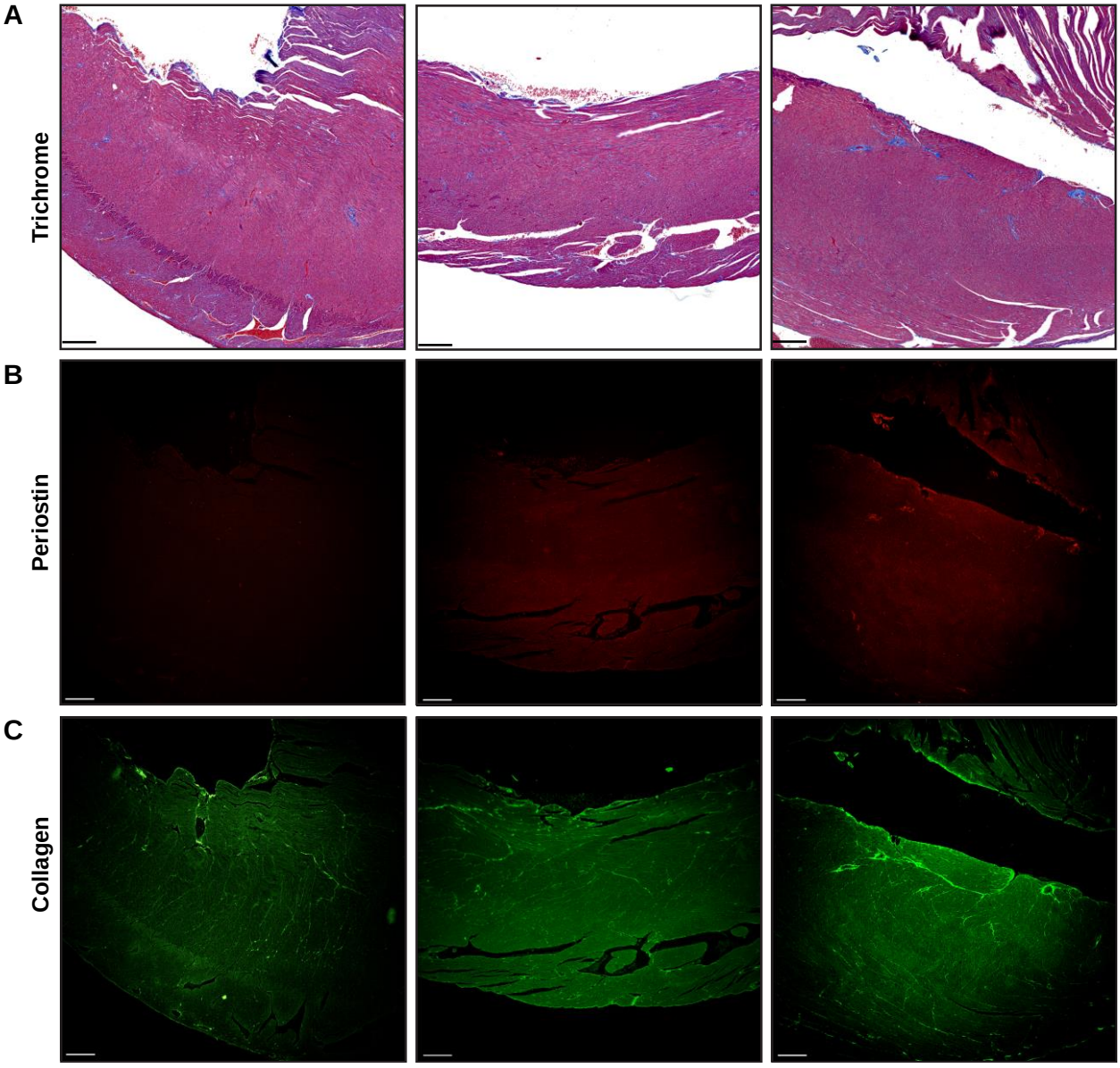

Supplemental Figure 3: The *Tfpi*$^{-/-}$*/Par4*$^{-/-}$ recipient mice did not have cardiac thrombosis or fibrosis prior to transplantation. The heart tissue from three *Tfpi*$^{-/-}$*/Par4*$^{-/-}$ mice was evaluated using (A) Trichrome stain, (B) periostin immunohistochemistry (fluorescent emission 647, red), and (C) Picrosirius red fluorescent stain (fluorescent emission 568, green) to delineate cardiac clot formation, fibroblast activation, and increased collagen production, respectively. No significant pathological lesions were observed (bar=100µm).

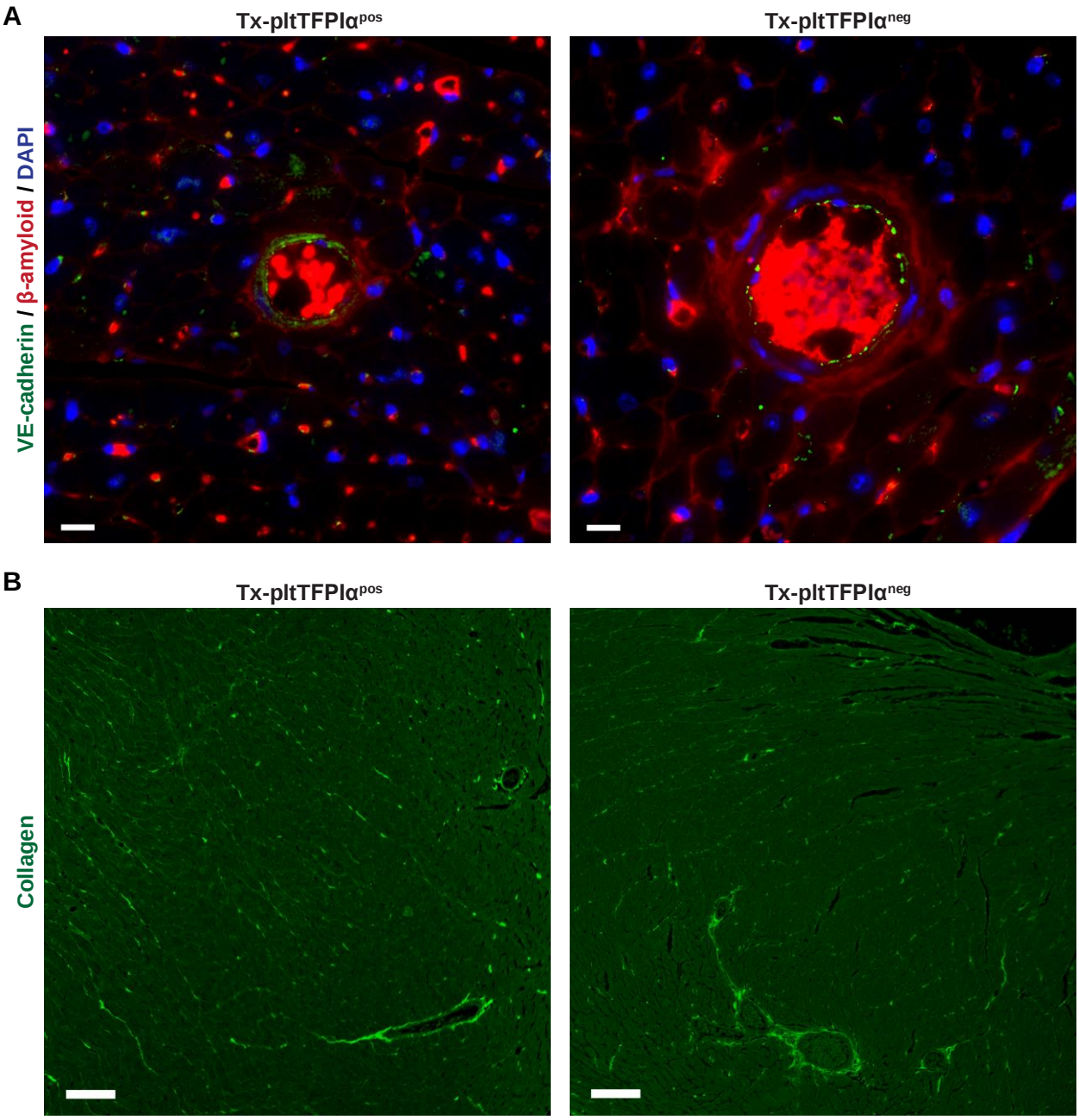

Supplemental Figure 4: Background radiation damage was evident by extravascular β-amyloid and low-level collagen deposition within Tx-pltTFPIα^{pos} and Tx-pTFPIα^{neg} hearts. **(A)** Immunolabeling of heart tissue with antibodies to detect extravascular plasma β-amyloid (red), endothelial VE-Cadherin (green), and DAPI nuclear counterstain (blue). The Tx-pltTFPIα^{pos} and Tx-pTFPIα^{neg} mice had β-amyloid leakage surrounding small arterioles that extended into the interstitium between the cardiac myocytes (bar=10μm). **(B)** Heart tissue was stained with pircosirius red to detect collagen with fluorescent emission at 568nm (green). The Tx-pltTFPIα^{pos} and Tx-pltTFPIα^{neg} hearts had low and equal amounts of radiation-induced collagen deposition indicated by the fluorescent staining located in perivascular areas and between the cardiomyocytes (bar=100μm).

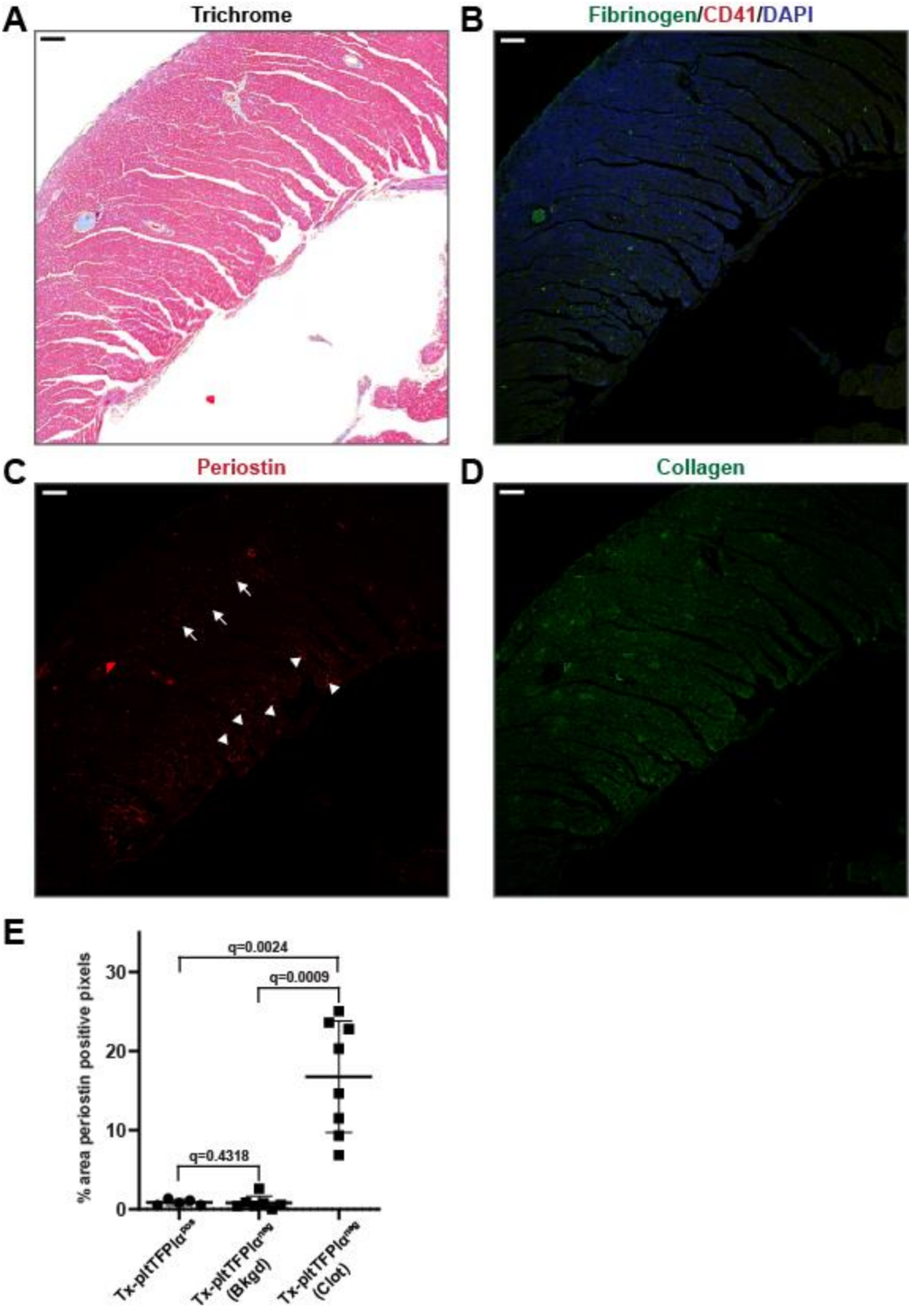
A
Trichrome
B
Fibrinogen/CD41/DAPI
C
Periostin
D
Collagen
E
% area periostin positive pixels
q=0.0024
q=0.0009
q=0.4318
30
20
10
0
Tx-pltTFPIα^Pos
Tx-pltTFPIα^neg (Bkgd)
Tx-pltTFPIα^neg (Clot)

Supplemental Figure 5: Tx-pltTFPIα^{pos} mice did not have ventricular thrombi. (A) Trichrome stain of a Tx-pltTFPIα^{pos} heart did not detect ventricular clots. **(B)** Tx-pltTFPIα^{pos} heart tissue was probed with anti-fibrinogen (green) and anti-CD41 (red) with DAPI nuclear counterstain (blue). These immunofluorescence images were negative indicating absence of fibrin and platelet deposition within the heart. **(C)** Immunofluorescence of periostin (red) in Tx-pltTFPIα^{pos} heart tissue. The arrows indicate presence of activated fibroblasts without periostin secretion, while arrowheads indicate presence of small amounts of periostin secreted into the ECM of tissue closest to the ventricular chamber. **(D)** Tx-pltTFPIα^{pos} heart tissue was stained with picrosirius red to detect collagen (green) (bar=100μm). **(E)** Periostin deposition in Tx-pltTFPIα^{pos} and Tx-pltTFPIα^{neg} hearts was quantified with Image J software. The Tx-pltTFPIα^{neg} clot-associated heart area was compared to non-clot associated background and the Tx-pltTFPIα^{pos} heart area.

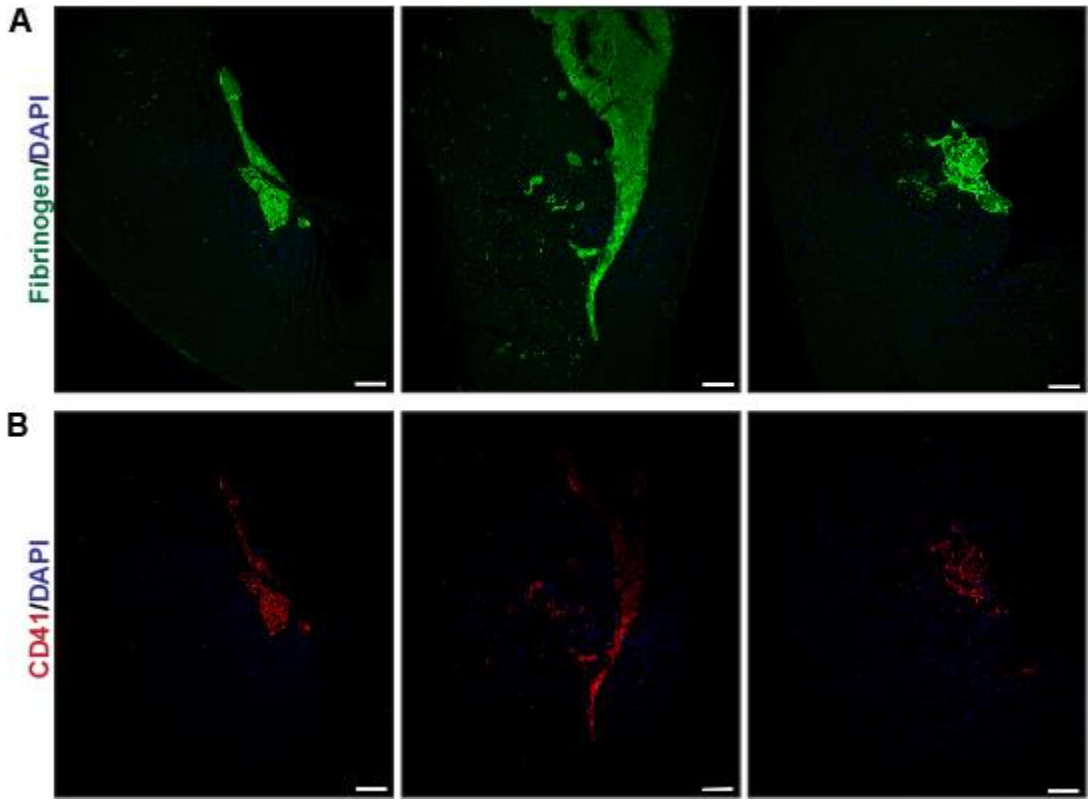

Supplemental Figure 6: Tx-pltTFPIα^{neg} cardiac thrombi were platelet and fibrin rich. Enlarged images of thrombi from the Tx-pltTFPIα^{neg} hearts in Figure 2D-F. The left and right panels display ventricular mural thrombi. The middle panel shows a large mural thrombus filling the right ventricle. **(A)** Tissue sections were probed with anti-fibrinogen (green) and **(B)** anti-platelet CD41 (red) with DAPI nuclear counterstain (blue). These images correspond with the merged images shown in Figure 3B.

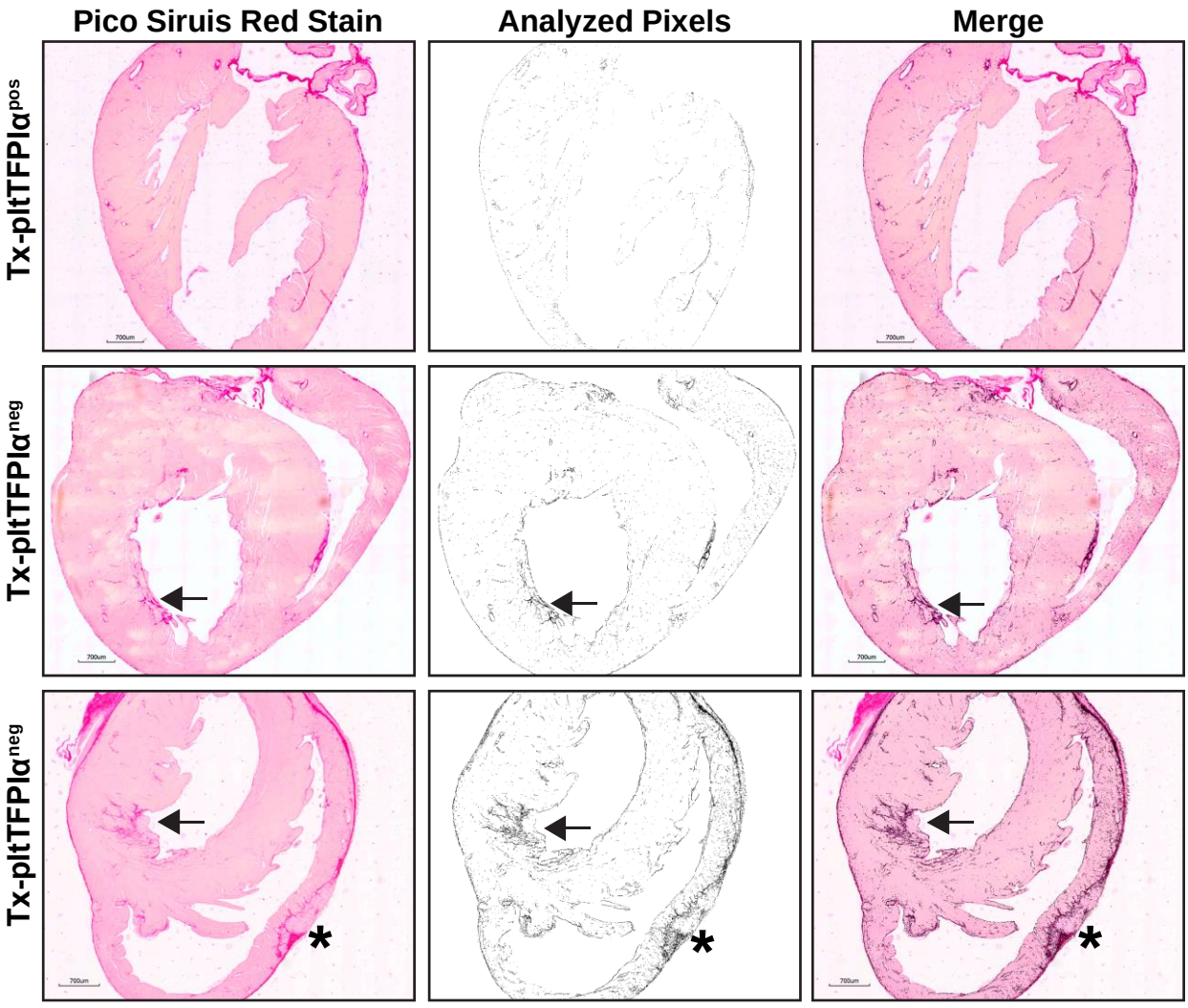

Supplemental Figure 7: Examples of heart images analyzed by Image J software.
The top row shows Tx-pltTFPIα^{pos} heart tissue. The bottom two rows show Tx-pltTFPIα^{neg} heart tissue. The tissues were stained with picrosirius red to detect collagen deposition within the heart (left). The Image J software generated an output of collagen deposition with increased pixel density correlating to areas of increased picrosirius red staining (middle). Merge of the picrosirius red stain and the Image J analyzed pixels (right) demonstrates the concentration of pixels at the ventricular mural thrombi (arrow) and within the heart muscle (asterisk). Bar=700µm.

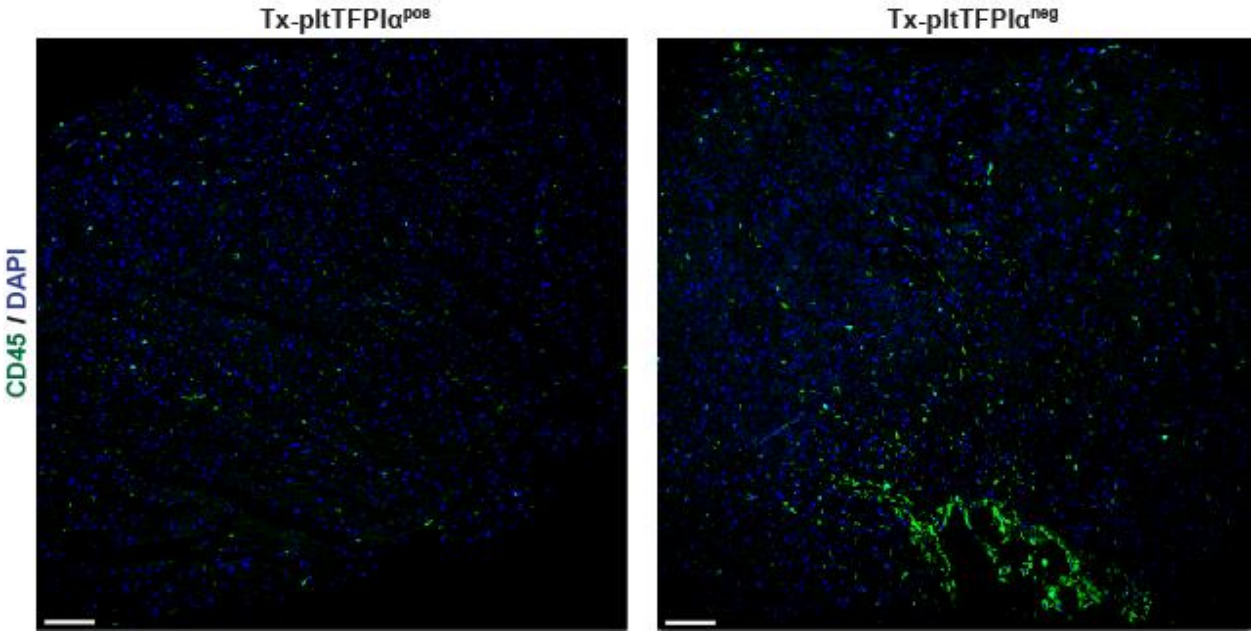

Supplemental Figure 8: CD45+ leukocyte infiltration into the ECM secondary to mural clot formation in Tx-pltTFPIα^{neg} hearts.
Immunoreactivity of CD45+ cells within the Tx-pltTFPIα^{pos} and Tx-pltTFPIα^{neg} heart tissue as demonstrated by green fluorescence using an anti-CD45 antibody and DAPI nuclear counterstain (blue) (bar=100µm).